Conf-780813--8

LA-UR-78-1191

MASTER

TITLE: UNSTEADY DETONATIONS DRIVEN BY FIRST-ORDER PHASE TRANSFORMATIONS

AUTHOR(S): R. L. Rabie and W. Fickett

SUBMITTED TO: High Dynamic Pressure Symposium
Paris, France

August 28 through September 1, 1978

By acceptance of this article for publication, the publisher recognizes the Government's (license) rights in any copyright and the Government and its authorized representatives have unrestricted right to reproduce in whole or in part said article under any copyright secured by the publisher.

The Los Alamos Scientific Laboratory requests that the publisher identify this article as work performed under the auspices of the USERDA.

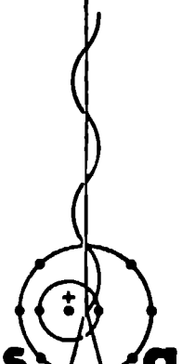

los alamos
scientific laboratory
of the University of California
LOS ALAMOS, NEW MEXICO 87544

An Affirmative Action/Equal Opportunity Employer

NOTICE
This report was prepared as an account of work sponsored by the United States Government. Neither the United States nor the United States Department of Energy, nor any of their employees, nor any of their contractors, subcontractors, or their employees, makes any warranty, express or implied, or assumes any legal liability or responsibility for the accuracy, completeness or usefulness of any information, apparatus, product or process disclosed, or represents that its use would not infringe privately owned rights.

UNITED STATES
ENERGY RESEARCH AND
DEVELOPMENT ADMINISTRATION
CONTRACT W-7405-ENG. 36

DISTRIBUTION OF THIS DOCUMENT IS UNLIMITED

UNSTEADY DETONATIONS DRIVEN BY FIRST-ORDER PHASE TRANSFORMATIONS

R. L. Rabie and W. Fickett
Los Alamos Scientific Laboratory, Los Alamos, New Mexico 87545, USA

G. R. Fowles
Washington State University, Pullman, Washington 99163, USA

Reactive waves supported by the energy released during a phase transformation are examined as elementary detonations. It is found that a class of eigenvalue detonations exist containing the well known Chapman-Jouguet solution as a particular case. In general the set of eigenvalue detonations are unsteady in any single inertial reference frame.

INTRODUCTION

A simple two-phase thermodynamic system possessed of a single first-order phase transformation is examined as an elementary explosive. The material is allowed to be viscous but not thermally conductive. A reaction rate and ignition condition are also assumed. This elementary system is sufficiently simple that analytic solution of the steady flow problem is possible and yet complex enough, due primarily to the including of viscosity, to show the effect of energy dissipation on the flow. The viscous flow problem for a conventional explosive is discussed in Detonation, for example.[1] It is qualitatively similar to that for the Navier-Stokes equations including viscosity, heat conduction, and diffusion, treated by Wood.[2]

The detonation solutions for our system have some features in common with the conventional viscous detonation, but differ in important ways. There are two possible solutions for unsupported detonation: the conventional, Chapman-Jouget (CJ) solution, and a new type of "eigenvalue" solution. Which one applies in a given case depends on both the material properties and the amount by which the initial state is displaced below the (equilibrium) phase transition pressure. The CJ solution lies entirely below the transition pressure. The eigenvalue solution consists of two waves, each steady in its own frame: the leading reactive shock and a slower following deflagration, or reactive rarefaction shock. Part of the reaction takes place in each wave, with the lengthening region between them a constant

equilibrium state. The complete-reaction state at the end of the deflagration is sonic, so that the following rarefaction is attached there as in the CJ detonation. The CJ detonation thus appears as a limiting case of an eigenvalue detonation when the leading compressive shock and the following rarefaction shock travel with the same speed.

Examples of metastable systems of the sort discussed here are numerous. The problem of emergency core cooling in nuclear reactors presents the possibility of super heating the coolant and thus the prospect of a vaporization wave. In geophysics, the mystery of the deep focus earthquake may be solved by considering the olivine/spinel transformation. Olivine carried below the phase boundary by convection becomes metastable and thus subject to self-sustaining transformation waves. Another example is crystallization waves in amorphous solids.

The following discussion is given in four sections. The first presents the governing equations as they are used in the remainder of the paper. The second section is a presentation of the analytic techniques used in examining the system together with the results of the analysis. The third contains the numerical calculations done to solve the time-dependent problem and the fourth is a discussion of the results of the entire investigation including possible applications.

I. THE GOVERNING EQUATIONS

The system is treated as a one-dimensional viscous fluid. The equation of continuity is

$$\dot{\rho} + \rho u_x = 0 \tag{1}$$

where ρ is the mass density and u is the particle velocity. The sub x refers to partial differentiation with respect to x at constant time and the superposed "$\cdot$" represents the convective or material derivative. The equation of momentum conservation is

$$\rho\dot{u} + \sigma_x = 0 \tag{2}$$

where σ is stress taken positive in compression. Energy conservation is given by

$$\dot{e} + \sigma\dot{v} = 0 \tag{3}$$

with $v = 1/\rho$ and e the internal energy per unit mass or specific internal energy. In addition to the conservation equations an equation governing the evolution of the reaction progress variable, λ, is required. The form assumed for this is

$$\dot{\lambda} = kr \tag{4}$$

where k is a constant of dimension t^{-1} and r is a dimensionless function of the thermodynamic state.

Equations (1)–(4) are supplemented by equations stating the constitutive assumptions made about the system. These assumptions are

$$\sigma = p + \pi \ , \tag{5}$$

$$\pi = -\nu u_x \ , \tag{6}$$

$$p(v,\lambda) = p_0(v_0^2/v^2) \ , \tag{7}$$

$$\bar{v}_0 = (1-\lambda)v_{01} + \lambda v_{02} \tag{8}$$

$$r(v,\lambda) = \begin{cases} (\lambda_{eq}(v) - \lambda) & \text{for } p \geq p_{ig} \\ 0 & \text{for } p < p_{ig} \end{cases} \tag{9}$$

and

$$\lambda_{eq}(v) = \begin{cases} 0 & \text{for } v < v_1^* \\ \dfrac{v-v_1^*}{v_2^*-v_1^*} & \text{for } v_1^* \leq v \leq v_2^* \\ 1 & \text{for } v > v_2^* \end{cases} . \tag{10}$$

In Eqs. (5) through (10) v_{01} and v_{02} are the values of the specific volume at pressure $p = p_0$ in the pure phases 1 and 2 respectively, ν is the coefficient of viscosity—taken to be constant—and v_1^* and v_2^* are the values of the volume at pressure $p = p^*$ (the constant phase transition pressure) in the pure phases 1 and 2 respectively. The quantity π is the viscous pressure and p_{ig} is the ignition locus, taken to be an isobar.

In the statement of the constitutive assumptions, Eqs. (5) through (10), a particular feature should be emphasized and this is the lack of temperature in Eq. (7). The p-v-T surfaces of phase 1 and phase 2 are shown in Fig. 1. The surfaces of constant λ in p-v-T space are sections of cylinders parallel to the T axis, that is, the coefficient of thermal expansion is set to zero. Another consequence of this is that Grüneisen's ratio is zero, which is admittedly unusual but not impossible. Finally, we have assumed a constant uniform specific heat and ideal mixing of specific internal energy and specific volume.

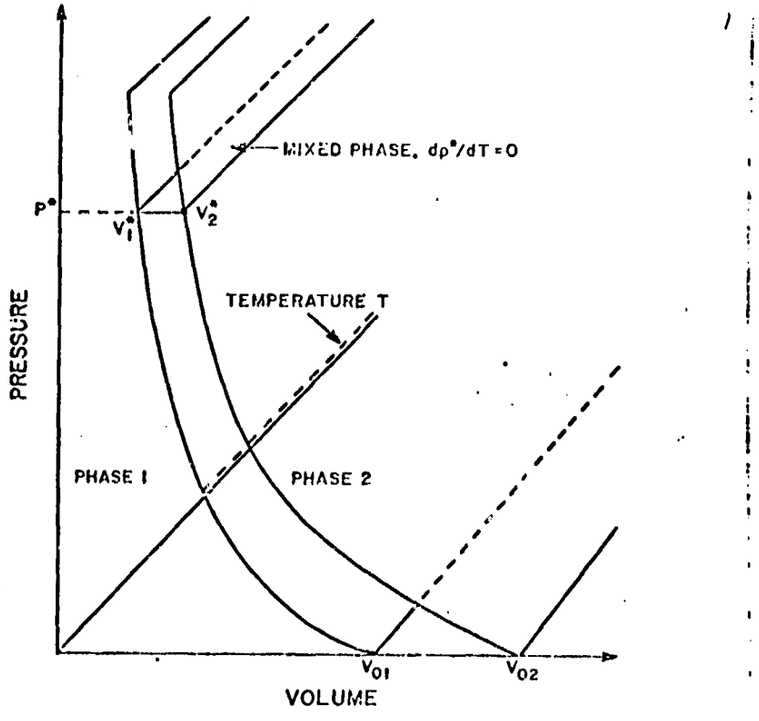

Fig. 1. P-V-T surfaces showing phases 1 and 2 and the equilibrium mixed phase.

The final equations to be recorded here are the equations for steady flow. These may be obtained from Eqs. (1) through (4) and they are, in the steady frame (whose velocity in the laboratory is D), given by

$$\rho(D-u) = \rho_0 D \quad , \tag{11}$$

$$\sigma - \sigma_0 = (\rho_0 D)^2 \ (v_0 - v) \quad , \tag{12}$$

$$e - e_0 = \frac{1}{2} (\sigma + \sigma_0) \ (v_0 - v) \quad , \tag{13}$$

and

$$u \frac{d\lambda}{dx'} = kr \tag{14}$$

where the prime denotes the steady frame and the sub "0" refers to the initial state assumed to be uniform and motionless.

II. THE STEADY PROBLEM

The general problem to be solved can be stated in the form of initial and boundary conditions for the equations of motion. Let the material be confined in a tube of semi-infinite length and perfectly slippery walls, closed at the left end by a massless piston, as shown in Fig. 2. The initial condition is the spatially uniform state $p = p_0$, $v = v_0$, $\lambda = \lambda_0 = 0$ with the *boundary pressure* p_b applied to the piston also equal to p_0 so that the piston remains at rest. The boundary condition is the specified pressure history $p_b(t)$ applied to the piston. For this we take the step function shown, with the applied pressure jumping at $t = 0$ to the constant boundary or piston pressure p_b. The initial jump initiates the detonation wave, and the constancy of p_b ensures that at least the rear part of the wave will eventually become steady.

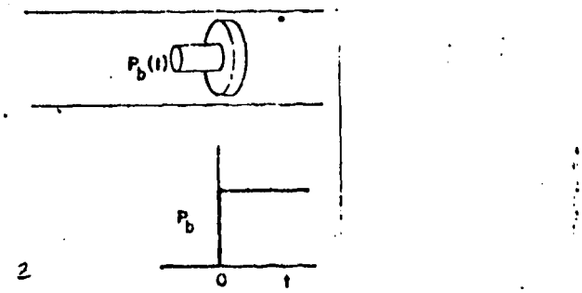

Fig. 2. The idealized experiment with input waveform.

This general problem has two mathematically distinct parts. The steady solutions—to be examined in this section—and time dependent behavior to be discussed in the following section.

The steady flow will be governed by Eqs. (5) through (14). By replacing σ in Eq. (12) with Eqs. (5) and (6) one gets

$$\nu \frac{du}{dx'} = (p - p_0) - (\rho_0 D)^2 \ (v_0 - v) = R \quad . \tag{15}$$

Equations (14) and (15) are a pair of autonomous differential equations for the steady flow. Using Eq. (11), they may be combined to form the equation governing the motion of the system point in the v-λ phase plane. This results in

$$L \frac{dv}{d\lambda} = \frac{vR(v,\lambda;D)}{r(v,\lambda)} \tag{16}$$

where

$$L = \nu k \quad .$$

The velocity, D, of the detonation wave occurs as a parameter in Eq. (16) that is to be adjusted to allow for a solution to a given piston problem. Figure 3 shows the relation between the common p-v plane representation of the problem and the v-λ phase plane of Eq. (16). Note that Eq. (16) has critical points wherever the loci R = 0 and r = 0 cross. The locus R = 0 is just the locus of steady wave equilibrium end states while the locus r = 0 is the zero rate curve. These two spaces are topologically equivalent; we shall describe how the loci of interest transform in going from p-v to v-λ. The constant-λ loci, or partial-reaction Hugoniots, not

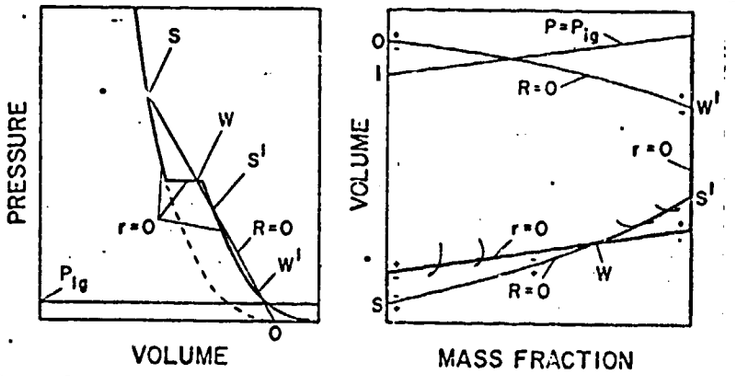

Fig. 3. The topological comparison of p-v and v-λ space.

shown, are just vertical straight lines in v-λ space. The line R = 0 is a straight line in p-v, with R > 0 above and R < 0 below. For the particular substance and value of D chosen for illustration, it intersects the equilibrium Hugoniot at four points, the strong points S and S' and the weak points W and W'. (We use the conventional terminology: The flow behind is subsonic with respect to the shock at a strong point and supersonic at a weak one.) In v-λ, the shape of the R = 0 line is like that of a left-opening parabola, with point S on the left boundary, points S' and W' on the right boundary, and point W in between. The function R is positive outside of R = 0 and negative inside, as indicated by the (+) and (-) signs next to the curve. The equilibrium Hugoniot, the solution of r = 0, has three branches: the upper branch with λ = 0, the transition region p = p*, and the lower branch with λ = 1. In v-λ, its upper and lower branches lie on the left and right boundaries, respectively. The transition region is the constant-pressure contour p = p* which intersects the R = 0 locus at point W. (The constant-pressure contours are segments of straight lines.) The function r is positive above r = 0 and negative below it, again indicated by (+) and (-) signs next to the curve. Finally, we have the ignition locus $p = p_{ig}$, another constant-pressure contour near the top of the v-λ diagram. It intersects the λ = 0 locus at the ignition point I. The vector field is readily sketched: The sign of the slope is that of R/r, and R = 0 and r = 0 are the loci of the horizontal and vertical turning points, respectively. The critical points are of course the intersections of these two loci, that is, points S, W, S', and W'. The shape of the vector field suggests that S and S' are nodes and W and W' are saddles. This turns out to be the case, as we shall shortly show. The points S' and W' occur in the conventional viscous detonation,[1] which we shall not discuss here. We will have some concern with point S', but not with point W'.

A few integral curves are shown in Fig. 4, with the direction of decreasing x (moving away from the initial state) indicated by arrows. The solution for a given D is the integral curve starting from the initial state at 0. Since our rate is zero for $p < p_{ig}$, the initial segment $\overline{0I}$ of the solution lies on the left boundary and is just the corresponding segment of

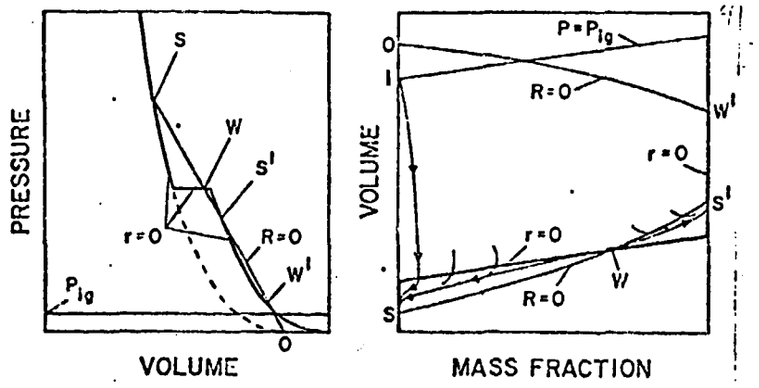

Fig. 4. Some integral curves and their behavior on r = 0 and R = 0.

the steady viscous nonreactive shock. When reaction begins at point I, the solution curve proceeds into the interior. For the case shown λ reaches a maximum as the curve crosses the r = 0 locus and v is a minimum as the curve crosses the R = 0 locus.

Thermodynamics and the Critical Points

A purely thermodynamic analysis of the behavior of the system in the vicinity of an interior critical point may be done by extending Gibbs' relation for reversible processes. The standard assumption is made that Gibbs' relation is also valid for first order deviations from equilibrium. This assumption together with Eq. (3) leads to

$$T\dot{s} = -(\sigma - p)\,\dot{v} - A\dot{\lambda} \tag{17}$$

where $A \doteq g_2(p,T) - g_1(p,T)$ is the difference in specific Gibbs energies or the affinity and s is the specific entropy. Assuming the strong form of the second law both terms on the r.h.s. of Eq. (17) must be positive. Employing standard thermodynamic identities it is possible to reduce Eq. (17) to the pair of conditions

$$(\rho_0 D)^2 + \frac{dp}{dv} \leq 0 \tag{18}$$

and

$$\left[\frac{dp}{dv} - \left(\frac{\partial p}{\partial v}\right)_{s,\lambda}\right]\left[\frac{dp}{dv} - \left(\frac{\partial p}{\partial v}\right)_{s,A}\right] \geq 0 \tag{19}$$

where $\frac{dp}{dv}$ is the slope of the integral curve in the limit as the critical point is reached.

The above thermodynamic analysis assumes that a unique solution to a given piston problem exists. Whether or not this is the case depends on the character of the interior critical points possessed by Eq. (16). To determine the character of the interior critical points a standard technique is employed.[3] This technique proceeds by expanding the numerator and denominator of the r.h.s. of Eq. (16) separately in the variables v and λ about the critical point. Denoting values at a critical point by a caret we have

$$L\frac{dv}{d\lambda} = \frac{a(v-\hat{v}) + b(\lambda-\hat{\lambda})}{c(v-\hat{v}) + d(\lambda-\hat{\lambda})}\,, \tag{20}$$

with

$$a = \frac{\partial(vR)}{\partial v}, \quad b = \frac{\partial(vR)}{\partial \lambda}, \quad c = \frac{\partial(r)}{\partial v}, \text{ and } \quad d = \frac{\partial(r)}{\partial \lambda} \ .$$

Our critical points are either nodes or saddles. The necessary condition for this is that the quantity $[(a-d)^2 + 4bc]$ be positive. Thus we get:

a node for $q > 0$

a saddle for $q < 0$

where

$$q = ad - bc \ .$$

The sign of q may be determined generally if the identification

$$\dot{\lambda} = - \ell A = kr \tag{21}$$

is made where ℓ and k are positive quantities and possibly functions of p and T. Equation (21) can be shown to hold near thermodynamic equilibrium and hence at all of our critical points. Employing Eq. (21) the quantity q may be shown to be

$$q = - \frac{\hat{v}\ell}{k} \left(\frac{\partial A}{\partial \lambda}\right)_{v,s} \left(\frac{\partial p}{\partial v}\right)_{A,s} \left[1 + (\rho_0 D)^2 \left(\frac{\partial v}{\partial p}\right)_{A,s}\right] \ . \tag{22}$$

The coefficient of this expression is always positive since thermodynamic stability requires

$$\left(\frac{\partial A}{\partial \lambda}\right)_{v,s} > 0 \text{ and } \left(\frac{\partial p}{\partial v}\right)_{A,s} < 0 \ .$$

Further, the quantity

$$(\rho_0 D)^2 \left(\frac{\partial v}{\partial p}\right)_{A,s} = - M_A^2$$

where M_A is the Mach number of the shock with respect to the material behind and with respect to the equilibrium (constant A) sound speed. In the specific problem treated in this paper $M_A = \infty$ in the equilibrium mixed phase and all interior critical points are saddles. The analysis for points on the pure phase boundaries is analogous if the entropy production is assumed to approach a maximum smoothly. With this one finds S and S' are nodes while W and W' are saddles.

The Eigenvalue Solution

The key to the entire problem is the eigenvalue solution, the integral curve from I which coincides with the separatrix of the saddle point W and thus passes into point W, veering neither to the left nor to the right. This happens only for a unique value of D, which we call $\hat{D}$, hence the name "eigenvalue". We call point W the *eigenvalue point*.

As D increases through $\hat{D}$, we have the sequence shown in Fig. 5. Note first that as D increases the R = 0 locus shifts to the right so that point W also moves to the right. For $D < \hat{D}$, Fig. 5a, the separatrix from point W intersects the $\lambda = 0$ axis below point I, and the solution veers off to the right, terminating at the lower strong point S'. For $D = \hat{D}$, Fig. 5b, we have the eigenvalue solution: The separatrix passes through point I and becomes

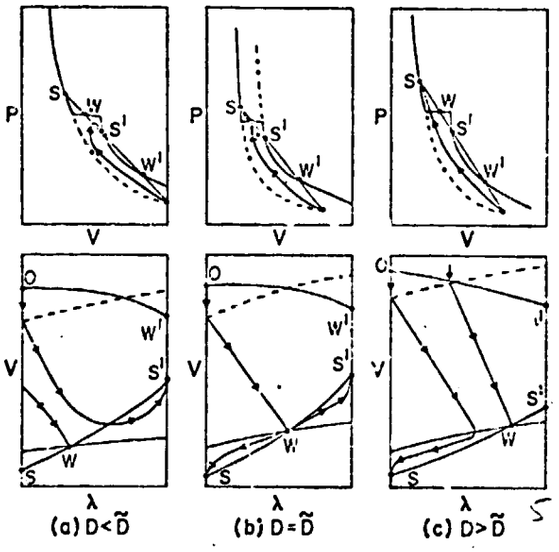

Fig. 5. The problem as a function of the wave velocity D.

the solution, which thus terminates in the upper weak point W. Finally, for $D > \tilde{D}$, Fig. 5c, the separatrix intersects the ignition locus to the right of point I, and the solution veers to the left of point W to terminate in the upper strong point S.

Double-Wave Solutions

In Fig. 5b there are two integral curves leaving W, one going to the left and terminating at S, and one going to the right and terminating in S'. Now the integral curve from I to W is a detonation terminating in the partially reacted equilibrium state W. The integral curves leaving W represent two possible following steady waves which can propagate into state W. These propagate at velocity $\tilde{D}$, the same as the leading wave $\overline{IW}$. The first wave $\overline{WS}$ (proceeding to the left in the phase plane) is an endothermic compression wave carrying the system back to the higher pressure no-reaction state S. The second wave $\overline{WS'}$ is a deflagration, carrying the system to the lower-pressure complete-reaction state S'.

Similar solutions in which the second wave (velocity D_2) runs slower than the first (velocity D_1) are also of interest. For these second waves we must draw a new v-λ diagram, Fig. 6, since we now have two different velocities $D_1 = \tilde{D}$ and $D_2 < \tilde{D}$. Figure 6 shows the two possible second waves

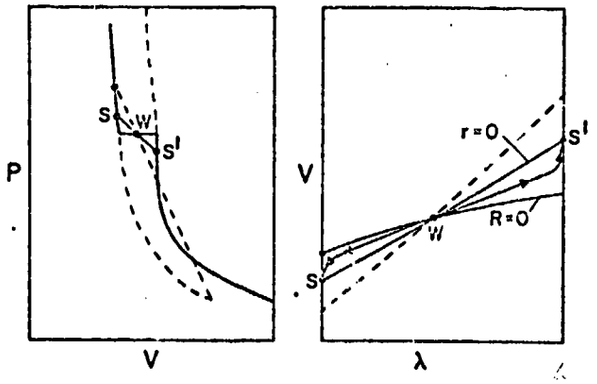

Fig. 6. The quasi-steady solutions in p-v and v-λ space.

of a particular velocity D_2. Here the Rayleigh line for the first wave and its extension to point S are shown dashed. The Rayleigh line for the second wave originates at point W. It is

$$R_2 = p - p_W - (\rho_W D_2)^2 \ (v_W - v) = 0 \quad ,$$

the solid line in the figure. The second waves are qualitatively the same as before, but they are weaker (point S is lowered and point S' is raised) and they run slower.

These double-wave solutions consist of two waves, each steady in its own frame, but moving at different velocities. There is, of course, no single frame in which the entire configuration is steady. We shall call such a configuration *quasi-steady*.

Effect of L

The effect of the material constant $L = k\nu$ is shown in Fig. 7. For the system defined by $p_0 = 1$ GPa, $v_0 = v_{01} = 1$ m^3/Mg, $v_{02} = 1.4$ m^3/Mg, $p^* = 5$ GPa, and $p_{ig} = 1.5$ GPa, we chose the value of $L = 5$ Mg m^{-1} s^{-1} to make $\tilde{\lambda}$ (the value of λ at p^* when $D = \tilde{D}$) about one-half. This gave $\tilde{\lambda} = 0.46$, $\tilde{D} = 2915$ m/s. With D fixed at this value we calculated integral curves for values of L ranging from 1 to 9 as shown. For this example the Rayleigh line lies entirely below the complete reaction locus in p-v so that the $R = 0$ locus does not intersect $\lambda = 1$ and points S' and W' are absent.

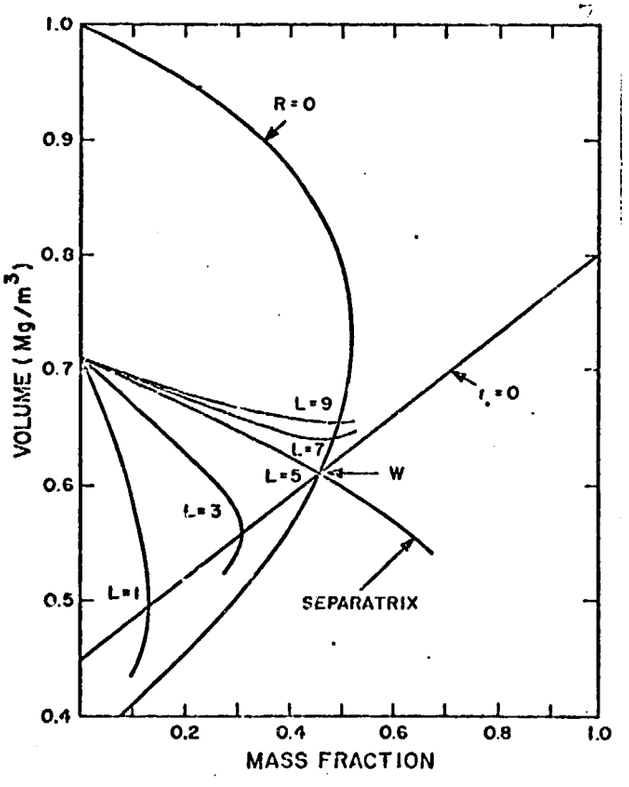

Fig. 7. The saddlepoint character of W.

In the following section the example calculated and displayed in Fig. 7 will be examined numerically. It is shown that the predictions of the foregoing analysis are borne out.

III. THE NUMERICAL EXPERIMENT

The finite difference[4,5] calculation to be displayed ir this section uses the equation of state and rate set out in Sec. I with the following constants

$$p_o = 1 \text{ GPa}$$
$$v_o = v_{01} = 1 \text{ m}^3/\text{Mg}$$
$$v_{02} = 1.4 \text{ m}^3/\text{Mg}$$
$$p^* = 5 \text{ GPa}$$
$$k = 1 \ \mu\text{s}^{-1}$$
$$p_{ig} = 1.5 \text{ GPa}$$
$$\nu = 5 \text{ GPa-}\mu\text{s} \ .$$

The problem consists of turning on a pressure boundary at time 0 at pressure 5 GPa. This is held for 1 μs and then released instantly to a value of 1 GPa. Figures 8 and 9 contain the essential numerical result. Figure 8 is a collection of four graphs of p vs x, u vs x, reaction extent vs x and ρ vs x at time 4.5 μs. Figure 9 shows the development and quasi-steady nature of the wave in a sequence of p vs x snapshots covering the time interval 0 to 5 μs. It is evident that the wave is self-supporting and quasi-steady.

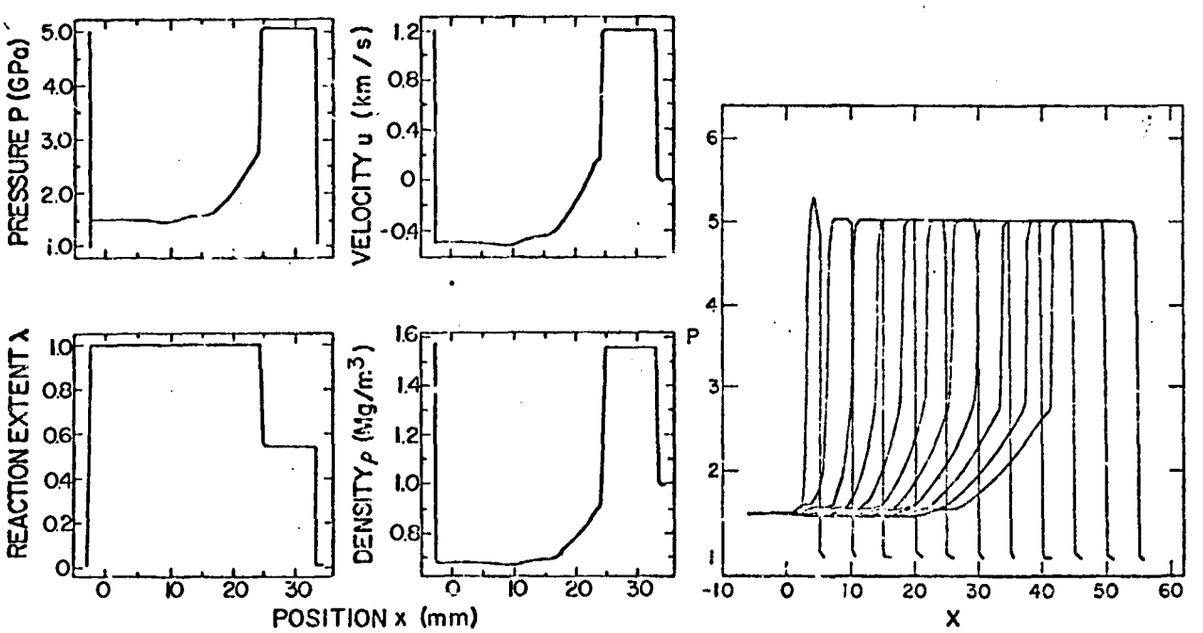

Fig. 8. Pressure, particle velocity, reaction extent, and density plotted against position for the quasi-steady unsupported wave.

Fig. 9. Pressure distance snapshots at various times showing growth of the quasi-steady wave.

IV. DISCUSSION

In the foregoing analysis it has been shown that the energy released during a phase transformation is capable of supporting detonation and deflagration waves that are only quasi-steady throughout the reaction zone. These results are general only to the extent that the simplifying assumptions made in this study do not alter the qualitative features of first-order phase transforming systems. For example, we have studied the α-quartz stishovite transformation in a simplified case and the results are quite similar to those obtained in this work. The question of general applicability, however, remains open.

The single most important question remaining to be answered is whether or not such waves as described in the preceding can exist. There is some experimental evidence suggesting that they do. recent work with supersaturated water vapor by D. R. Forshey and W. A. Courtney being an example.[6] Another possibly related phenomena is the "explosive" crystallization of amorphous solids. Both arsenic and germanium have shown such behavior.[7,8]

References

1. W. Fickett and W. C. Davis, Detonation, (University of California Press, Berkley, 1978) in press.
2. W. W. Wood, Phys. Fluids 6, 108 (1963).
3. G. Birkhoff and G. Rota, Ordinary Differential Equations (Blaisdell, Waltham, Mass. 1969), Ch. 5.
4. W. Fickett, Los Alamos Scientific Laboratory report LA-6859-MS (1977).*
5. W. Fickett, Los Alamos Scientific Laboratory report LA-5910-MS (1975).*
6. D. R. Forshey and W. G. Courtney, Bureau of Mines report RI 8256, 1977.
7. Von Sonja Geisling and Hans Richter, Acta Crystallogr. 2, 305 (1949).
8. R. Messier, T. Takamori, and R. Roy, Solid State Communications 16, 311 (1975).

* This report is available from National Technical Information Service
U. S. Department of Commerce
5285 Port Royal Road
Springfield VA, USA, 22161

Figure Captions

Fig. 1. P-V-T surfaces showing phases 1 and 2 and the equilibrium mixed phase.

Fig. 2. The idealized experiment with input waveform.

Fig. 3. The topological comparison of p-v and v-λ space.

Fig. 4. Some integral curves and their behavior on $r = 0$ and $R = 0$.

Fig. 5. The problem as a function of the wave velocity D.

Fig. 6. The quasi-steady solutions in p-v and v-λ space.

Fig. 7. The saddlepoint character of W.

Fig. 8. Pressure, particle velocity, reaction extent, and density plotted against position for the quasi-steady unsupported wave.

Fig. 9. Pressure distance snapshots at various times showing growth of the quasi-steady wave.